JOURNAL OF APPLIED ELECTROCHEMISTRY 24 (1994) 18–29

Solderability assessment via sequential electrochemical reduction analysis

D. MORGAN TENCH, D. P. ANDERSON, P. KIM

Rockwell International Science Center, Thousand Oaks, CA 91360, USA

Received 8 October 1992; Revised 20 February 1993

A recently-developed sequential electrochemical reduction analysis method permits nondestructive assessment of solderability loss associated with surface oxides on metals and can be applied to almost any part geometry, including printed wiring board through-holes and surface pads. Preliminary results indicate that metal sulphides can also be detected, at least in some cases. The type and amount of oxides detected for tin coatings are shown to correlate with solderability determined by the wetting balance method. The data indicate that formation of excessive amounts of SnO_2 in the surface oxide is a primary cause of Sn solderability degradation.

1. Introduction

Chronopotentiometry was apparently applied to analysis of oxides on metals (iron, copper and silver) for the first time in the 1930s [1, 2], and was subsequently developed as a means for quantitative detection of oxides on tin [3–8]. Recently, this work has been extended to the development of a chronopotentiometric method for assessing solderability loss caused by metal oxidation [9], which is an important problem that costs the electronics industry millions of dollars annually. Since the latter method involves reduction of surface oxides (and other species) in sequence to provide a quantitative measure of both the type and amount of each oxide present, it has been termed sequential electrochemical reduction analysis (SERA^{TM}).

In the present paper the important considerations in applying the SERA method are discussed. Wetting balance and SERA data obtained for copper wires with a hot-dipped pure tin finish are used for purposes of illustration since such specimens can be reproducibly oxidized electrochemically to provide standard surfaces for comparison. These data are also germane to Sn–Pb surfaces at which Sn oxides predominate because tin migrates to the surface along grain boundaries and is preferentially oxidized [10–12]. The SERA method can be applied to other metals, e.g. copper, and can be used to detect other surface species that affect solderability, e.g. sulphides.

2. Procedure

In the SERA method, the part to be analysed is brought in contact with an electrolyte chosen to facilitate reduction and minimize chemical dissolution of the oxides of interest. A constant cathodic current is applied between the part and an inert counter electrode (e.g. platinum or stainless steel) and the cathode potential is monitored as a function of time relative to a reference electrode. With this three-electrode arrangement, the potential of the cathode can be monitored without concern about changes in the anode potential. The applied current is chosen to avoid excessive polarization of the cathode and is typically very small ($< 100\,\mu A\,cm^{-2}$) so that the voltage drop in the bulk electrolyte is negligible. The electrolyte must be deaerated (via purging with an inert gas) since electrochemical reduction of oxygen would otherwise interfere with the analysis. It is also necessary to prevent oxygen generated at the anode by electrolysis of water from reaching the cathode during the measurement, either by placing the anode far from the cathode or using a porous glass frit to form a diffusion barrier.

2.1. *Oxide reduction potentials*

Equilibrium potentials calculated from thermodynamic stability data set the positive limits for reduction of the various species present. Table 1 gives the values for reduction of the more stable oxides and hydroxides of tin, lead, copper, silver, iron and nickel [13] to the respective metals at pH 8.4 (that of the borate buffer electrolyte used in the present work) according to reactions typified by:

$$SnO + 2H^+ + 2e^- = Sn + H_2O \quad (1)$$

$$Sn(OH)_2 + 2H^+ + 2e^- = 2H_2O \quad (2)$$

All of these voltages exhibit a pH dependence of -0.0591 V per pH unit. For tin, lead and copper, the difference in equilibrium potential for complete reduction of the oxide compared to the hydroxide (hydrated form) is very small (< 40 mV) except for $Sn(OH)_4$ whose reduction potential of -0.746 V is 0.1 V positive of that for SnO_2 (-0.844 V). Note that $Sn(OH)_4$ can also be reduced to either $Sn(OH)_2$ or SnO at more positive potentials (about -0.65 V) but

0021-891X

Table 1. Equilibrium voltages vs SCE for complete reduction of various oxides and hydroxides at pH 8.4

AgOH	0.767	Ag_2O	0.435
$Cu(OH)_2$	−0.129	CuO	−0.168
		Cu_2O	−0.267
$Pb(OH)_2$	−0.461	PbO	−0.488
$Ni(OH)_2$	−0.622	NiO	−0.628
		FeO	−0.785
		Fe_3O_4	−0.823
$Fe(OH)_3$	−0.679	Fe_2O_3	−0.789
$Sn(OH)_2$	−0.829	SnO	−0.842
$Sn(OH)_4$	−0.746	SnO_2	−0.844

is thermodynamically unstable with respect to SnO_2 and would not be formed under ambient conditions [14].

Because of kinetic factors, actual reduction potentials are generally more negative than predicted from thermodynamic considerations and depend on the applied current density. The potential ranges for reduction of Cu and Pb oxide species in pH 8.4 borate buffer are usually −0.3 to −0.6 V and −0.5 to −0.6 V, respectively. Although the equilibrium potentials for the Sn(II) and Sn(IV) species are practically equivalent, reduction of the latter is particularly inhibited kinetically and occurs at much more negative potentials, as discussed below. Thus, tin oxides/hydroxides are reduced over the broad range from −0.85 to −1.3 V vs SCE.

2.2 *SERA curve features*

Figure 1 schematically illustrates the features normally observed for SERA curves of electrode potential against time, and delineates the voltage regions for the various oxides pertinent to Sn–Pb coatings on copper substrates. For the ideal case involving well-defined surface compounds that are all exposed to the electrolyte (solid curve), the cathode voltage initially decreases to a plateau corresponding to reduction of the most easily reduced oxide. After the latter is completely reduced, the voltage again decreases to the value required for reduction of the next oxide. This process is repeated until all oxides are reduced and a steady voltage corresponding to hydrogen evolution from water electrolysis is attained. An analogy is the heating of ice water for which the temperature remains constant until the ice melts, and then increases to the boiling point of water where it again remains constant until all of the water has evaporated.

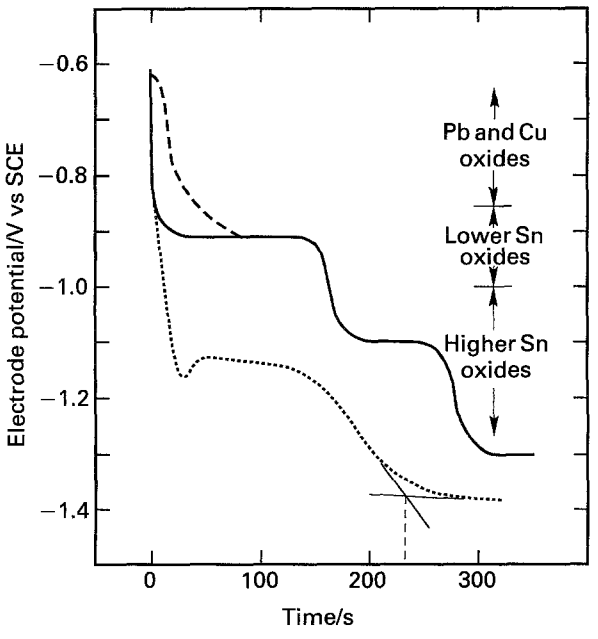

Fig. 1. Schematic illustration of ideal and normally-observed SERA curve features.

For each SERA plateau, the voltage identifies the type of oxide and the associated charge density (current density × time) yields a measure of the amount present. As indicated in Fig. 1, the point of complete oxide reduction may be taken as the intersection between extrapolations of the steepest part of the curve (in the transition region) and the plateau for the next oxide. This procedure was used in the present work but the point of maximum voltage change determined by differentiation of the SERA curve provides comparable results. For uniform, nonporous oxides of known chemical composition, the oxide thickness can be calculated but it is less ambiguous to utilize charge density as a measure of the oxide amount in making comparisons.

In practice, SERA curves are often distorted since surface oxides may be comprised of ill-defined compounds, intimate mixtures, and/or layers, and all species may not be exposed to the electrolyte initially. For example, oxides formed on Cu–Sn intermetallics apparently involve intimate mixtures of Cu and Sn oxide species since such compounds exhibit ill-defined SERA waves in both the Cu and Sn oxide potential regions [9]. Since Pb oxides usually do not form on Sn–Pb surfaces [10, 15–17] that are not severely depleted in tin, the presence of a shoulder positive of −0.8 V in SERA curves for Sn–Pb (or tin) coatings on copper (dashed curve in Fig. 1) is indicative of exposed/oxidized Cu–Sn intermetallic. A negative voltage peak (dotted curve in Fig. 1) indicates the presence of a duplex oxide structure, typically comprised of an outer layer that is more difficult to reduce electrochemically but once removed allows reduction of the more easily reduced underlayer to proceed (at less negative potentials). The dotted curve in Fig. 1 also illustrates the sloping plateau, negative shift in plateau voltage, and tailing that are typical of intimate oxide mixtures.

Because a mixture of species having differing effects on solderability is often involved, it is convenient to classify Sn oxide films as 'lower' or 'higher' oxides (see Fig. 1). As discussed below, the lower Sn oxide is reduced relatively easily, between −0.85 and −1.0 V vs. SCE, and is predominately SnO which exerts a relatively minor effect on solderability (at least when not excessively thick). The higher Sn oxide reduces between −1.0 and −1.4 V and contains appreciable amounts of SnO_2, which is a good thermal/electrical insulator [18] and is highly detrimental to solderability.

Table 2. Hydrogen evolution potentials (vs. SCE) at $-20\,\mu A\,cm^{-2}$ for various metals in borate buffer solution (pH 8.4)

Palladium	−0.57
Platinum (99.95%)	−0.71
Nickel (Ni-200)	−0.87
Gold	−0.90
Kovar	−0.95
Copper–beryllium alloy	−0.95
Carbon steel (1018)	−0.96
Stainless steel (304)	−1.00
Copper (OFHC)	−1.05
Copper (resistor wire)	−1.06
Silver (99.9%)	−1.06
Titanium (Ti-6V-4Al)	−1.18
Brass	−1.20
Eutectic tin–lead	−1.25
Tin (99.999%)	−1.27
Copper–tin intermetallics	−1.32
Aluminium (3003)	−1.33
Lead (99.95%)	−1.35

2.3. *Hydrogen evolution effects*

Species requiring very negative potentials for reduction may not be completely reduced before the onset of hydrogen evolution (water electrolysis). Current associated with the latter, which is thermodynamically possible negative of −0.74 V vs SCE in pH 8.4 solution, would introduce an error so that the amount of oxide determined from the charge passed would be too high. Most metals are not very effective proton reduction catalysts so that hydrogen evolution on their surfaces requires additional negative voltage (overvoltage), which extends the voltage range available for oxide reduction.

Table 2 gives the steady-state hydrogen evolution potentials measured at $-20\,\mu A\,cm^{-2}$ in pH 8.4 borate buffer solution for various metals. The results for untreated metals and those etched to remove the native surface oxide were comparable. Fortunately, copper oxides are relatively easy to reduce and the hydrogen overvoltages for tin, lead and the copper–tin intermetallics are relatively high so that most oxide species can be fully reduced on their surfaces. However, when the cathode comprises two metals with differing hydrogen overvoltages (as an electrical contact or because of exposure of the basis metal through a coating), the effect of the lower overvoltage metal on the analysis should be considered.

The hydrogen overvoltages for oxides are often higher than for the corresponding metal so that a steady-state hydrogen evolution potential for SERA analysis that is more negative than expected may be indicative of unreduced oxide residues (see Fig. 1). On the other hand, changes in substrate surface roughness will affect the actual current density and thus the final potential attained. In practice, the hydrogen evolution potentials for Sn–Pb coatings are found to vary between −1.25 and −1.4 V, presumably reflecting the interactive effects of surface roughness, grain structure (which ranges from fine to coarse), and Sn/Pb ratio.

2.4. *Current density effects*

The current density used for SERA analysis should be optimized to provide good resolution and accuracy, and a reasonably short analysis time. As the current density is increased, SERA features tend to shift toward more negative voltages and become less distinct because reduction processes are perturbed further from equilibrium and may not be able to respond sufficiently fast. At excessive current densities, plateau voltages may be too ill-defined for proper oxide characterization and the voltage may be driven to the next plateau before oxide reduction is complete so that the amount of oxide measured is too small. On the other hand, a very low current density may include appreciable contributions from reduction of residual oxygen and solution impurities so that the measured oxide amounts are too large. Note that total elimination of oxygen in a practical test system is difficult to attain.

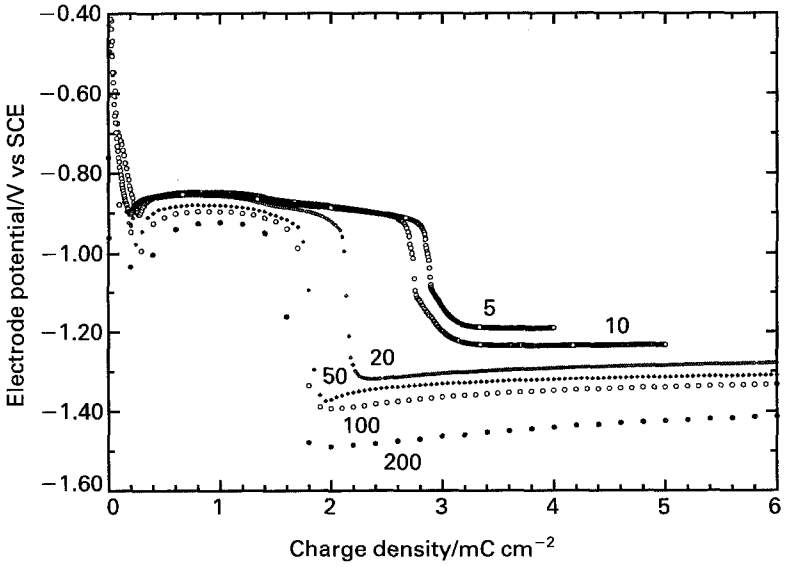

Fig. 2. SERA curves at various current densities for hot-dipped tin specimens anodized at $20\,\mu A\,cm^{-2}$ to a voltage of 0.4 V vs SCE.

These points are illustrated by the SERA curves for tin specimens anodized to 0.4 V shown in Fig. 2. For current densities of -5, -10 and $-20\,\mu A\,cm^{-2}$, the initial voltage dip and plateau are practically constant and a subtle plateau, whose voltage is only slightly more negative, is resolved. The curves for -5 and $-10\,\mu A\,cm^{-2}$ indicate a significantly larger total amount of oxide and exhibit much more positive hydrogen evolution potentials that may be attributable to interference from background currents, suggesting that these current densities are too low. On the other hand, as the magnitude of the cathodic current density is increased appreciably above $20\,\mu A\,cm^{-2}$, all of the curve features shift toward more negative voltages and become less distinct, and the indicated amount of oxide is less. In addition, the voltage exhibits a negative peak in the hydrogen evolution region and then slowly increases with time, suggesting slow reduction of residual oxide not reduced in the oxide plateau region. This effect is not pronounced at $-20\,\mu A\,cm^{-2}$, which appears to be nearly optimal for analysis of tin surfaces.

The current density effects depicted in Fig. 2 are actually much more pronounced than those observed for tin oxides formed under ambient conditions, for which the SERA oxide features are practically unchanged from -20 to $-100\,\mu A\,cm^{-2}$ and the hydrogen evolution potential remains constant. This is not surprising since perturbation of the surface region far from equilibrium via accelerated aging would be expected to produce thicker and more distinct oxide phases that are difficult to reduce, especially when an electrically-insulating species is involved. Consistent with this explanation, tin specimens mildly anodized to -0.2 V (instead of $+0.4$ V) yield SERA curves that are independent of current density from -20 to $-100\,\mu A\,cm^{-2}$, except for the expected small increase in the hydrogen evolution overvoltage.

For the present work, which involved tin specimens anodized under a variety of conditions, a SERA current density of $-20\,\mu A\,cm^{-2}$ was used. At the more positive anodization potentials, some residual oxide was undoubtedly omitted from the analysis but the amount was probably always small (submonolayer) and did not introduce a significant error since wetting balance tests of SERA-reduced specimens consistently gave very short wetting times. In any case, SERA analysis should provide an accurate indication of the type of oxide present and a relative measure of the oxide amount. Our results for both tin and Sn–Pb indicate that the nature of the oxide is more important to solderability than the amount, at least when the oxide is not excessively thick. For naturally-aged specimens, SERA oxide analysis is apparently quantitative.

3. Experimental details

All electrochemical experiments were performed in argon-saturated pH 8.4 borate buffer solution ($9.55\,g\,dm^{-3}$ sodium borate and $6.18\,g\,dm^{-3}$ boric acid), which provides minimal solubility for tin oxides

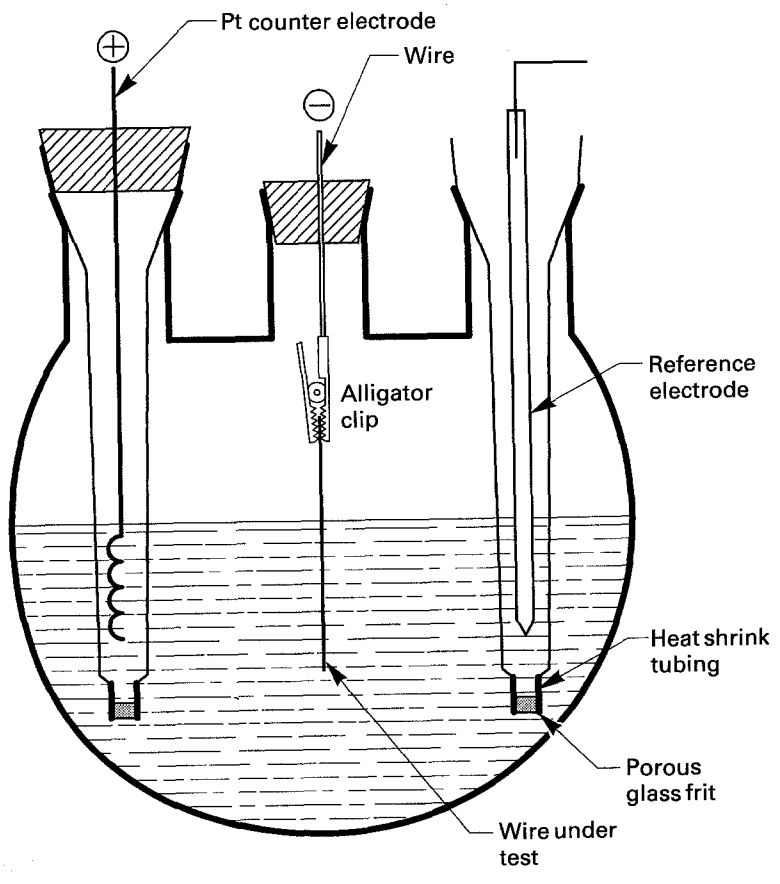

Fig. 3. Electrochemical cell used for SERA testing wire specimens.

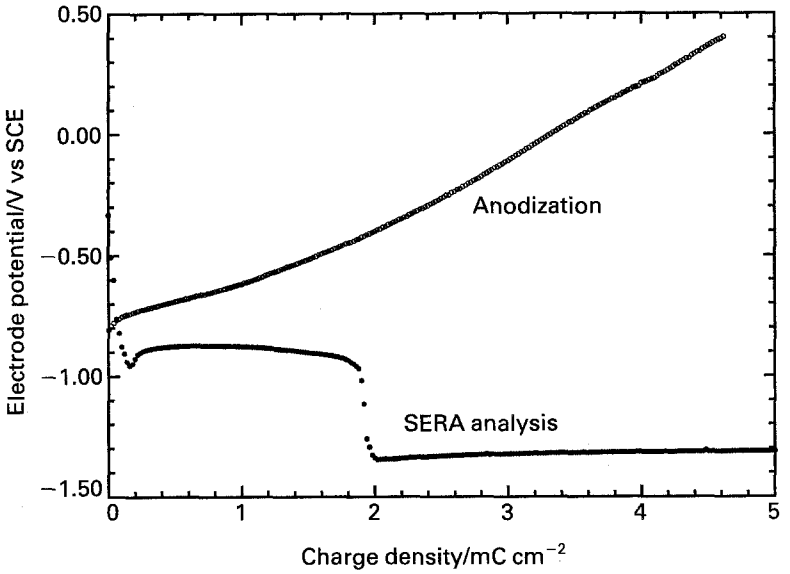

Fig. 4. Chronopotentiograms at 20 μA cm^{-2} for anodization to 1.0 V, and SERA analysis of tin specimens in deaerated borate buffer solution.

[19]. As illustrated schematically in Fig. 3, the glass cell was a round bottom flask that contained 200 ml of electrolyte and had five necks (only three shown), all with standard taper joints. To minimize electrolyte contamination by oxygen and chloride, the platinum counter electrode and reference saturated calomel electrode (SCE) were contained in separate compartments (glass tubes) electrically connected to the main compartment via porous Vycor glass disks (sealed to the tube ends with heat-shrink teflon tubing). Specimens were held partially immersed in the electrolyte by an alligator clip (above the electrolyte level) connected to a copper rod that was press-fitted through a rubber stopper (which never contacted the solution). Argon was continuously bubbled through the electrolyte via a gas dispersion tube (not shown in Fig. 3) and was vented into an argon atmosphere glove box in which all electrochemical experiments were performed.

Unless otherwise noted, a current density of 20 μA cm^{-2} was used for all reductions and anodizations. Constant current was applied via a Keithley Instruments Model 224 programmable current source and the electrode potential was followed via a Fluke Model 8842 multimeter. Chronopotentiograms were recorded under computer control using an Apple Macintosh II desktop computer with a National Instruments 16-bit multipurpose IO board (Model NB-MIO-16).

Hot-tin-dipped test specimens were prepared by dipping bare copper resistor wire (0.8–0.9 mm dia. × 8 cm long) to a depth of 3 cm in molten tin at 288 °C. Prior to being hot dipped, the wires were immersed in water soluble flux (Ardrox PC234M) for 5 s and excess flux was removed by touching the wire end to laboratory tissue. Finished wires were rinsed with deionized water at approximately room temperature.

Specimens having a reproducible surface oxide structure were prepared by constant current anodization at 20 μA cm^{-2} in deaerated pH 8.4 borate buffer solution. Since even a small amount of residual oxide was found to affect the reproducibility of SERA and wetting balance results, specimens were fully-reduced prior to anodization. This is consistent with the findings of Shah and Davies [20], who found that tin dissolution at tin anodes in borate buffer is inhibited if the air formed oxide is not reduced prior to anodization. Oxide removal in the present work was accomplished by a 30 s exposure in a 0.8 M chromous sulphate solution (pH 0.5) prepared by reduction of the chromic species at a lead cathode in a glass cell under an argon atmosphere, with the platinum anode in a separate compartment isolated by porous Vycor glass. The chromous ion treatment was also performed inside the argon atmosphere glove box and the specimen (after being rinsed in deionized water) was transferred immediately to the anodization/analysis cell. SERA analyses after the reduction treatment always indicated that the amount of oxide remaining was negligible.

Figure 4 gives chronopotentiograms that illustrate the method used to prepare and analyze oxidized tin specimens. During 'anodization', the voltage exhibited an ill-defined arrest at about −0.7 V and then increased monotonically to the final value (0.4 V in this case). The subsequent 'SERA analysis' was performed in the same solution. Considerable variation was observed in the anodization curves but the SERA curves for a given voltage limit were very reproducible. The specimen was then re-anodized to the same voltage and, after being rinsed in deionized water and blown dry with argon, was tested on a wetting balance using an unactivated rosin (R) flux (Kester Formula 135).

To minimize the effects of sporadic experimental deviations, five specimens were tested for each set of conditions and the highest and lowest values were disregarded in all cases. The standard deviation for the three total oxide measurements was always less than 10%, and for the three wetting balance measurements was less than 10% except for anodization voltages of 0.3 and 0.9, for which it was 20%. Use of

all five points gave almost identical results except that the standard deviation was somewhat higher in some cases.

The wetting balance was a Multicore universal solderability tester controlled by an IBM Model XT personal computer. Wetting curves of force against time were recorded at 100 points per second using a modified computer program obtained from National Standard Corporation. Measurements were made with the solder pot at either 235 or 295 °C. The wetting time was taken as the time required to reach 2/3 of the maximum theoretical wetting force of 400 [21]. This choice, rather than the time to 2/3 of the maximum force attained, avoids the possibility that a poorly wettable specimen would exhibit a short wetting time.

Most materials used to measure hydrogen overvoltages in the deaerated borate buffer solution were first etched in aqueous solutions of either 3 M nitric acid (Pt, Au, Cu-Be, Cu, Ag, brass, Cu–Sn intermetallics), 1 vol % hydrogen peroxide/8 vol % fluoroboric acid (Sn–Pb, Sn, Pb), or 1 vol % conc. nitric acid/1 vol % conc. hydrofluoric acid (Ni, steels). In most cases, unetched specimens gave comparable results. The specimen configurations were: foils or sheets for Ti, Al, Pd, OFHC Cu, and the steels; bars for brass and Sn–Pb; a tube for Kovar; and thin wires for all other materials. A partially submerged area of 0.5 to 7 cm^2 was used for the measurement. A constant current of $-20\ \mu A\ cm^{-2}$ was applied until a steady voltage plateau was observed.

Specimens exposed to H_2S were suspended above a mixture of Na_2S and concentrated HCl in an Erlenmeyer flask.

4. Tin results and discussion

As mentioned above, hot tin dipping of copper wires was found to sometimes produce recalcitrant tin oxide layers that had to be removed in order to obtain reproducible results. Commercial tin foil specimens (simply vapour degreased in benzene or etched in 3 M nitric acid solution), on the other hand, did not require prereduction in chromous solution, indicating that the oxide layer in this case is removed

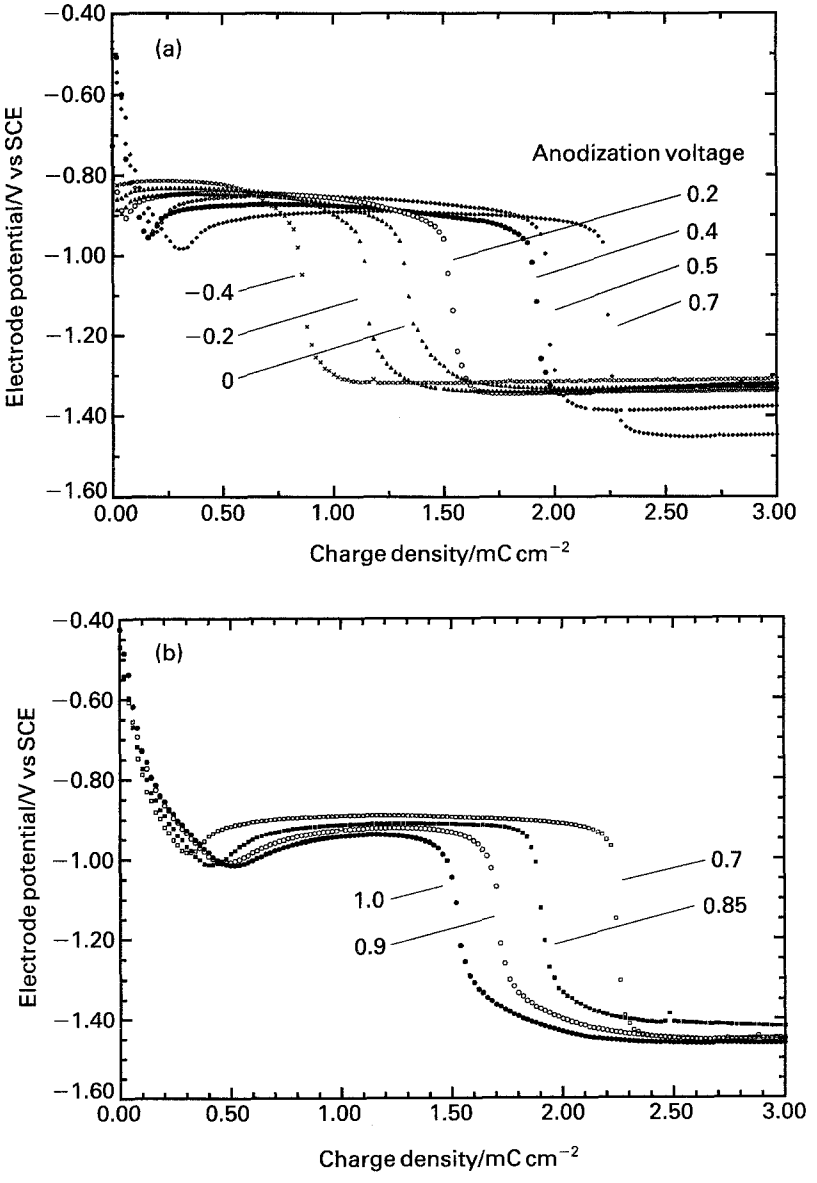

Fig. 5. SERA curves for hot-dipped tin specimens anodized at $20\ \mu A\ cm^{-2}$ to various voltage limits: (a) −0.4 to 0.7 V and (b) 0.7 to 1.0 V.

completely by reduction in the borate buffer solution. Nonetheless, after removal of surface oxides, the behaviour of the two types of specimens was found to be comparable.

Figure 5 shows SERA curves obtained for hot-dipped tin specimens anodized to various voltage limits. Up to 0.2 V, the curves indicate the presence of only one oxide (single plateau), the amount of which increases with the anodization limit. This oxide is apparently an Sn(II) species, SnO or $Sn(OH)_2$, which has been reported to form under mildly oxidizing conditions by various authors [e.g. 20]. As the anodization voltage limit is increased further, a negative voltage dip becomes evident and the voltage plateau shifts toward more negative values. For oxides formed at 0.7 V and more positive potentials, the hydrogen evolution plateau becomes more negative, indicating a fundamental change in the nature of the oxide and the presence of residual oxide after the SERA analysis. As the anodization potential is increased above 0.7 V, the total amount of oxide detected by SERA analysis decreases.

These results are comparable to those obtained by Shah and Davies [20] who studied oxidation of tin foil in 0.5 M sodium borate (pH 9.3). They found (by turbidimetric analysis of the solution) that for anodization limits up to 0.2 V exactly half of the current goes toward tin dissolution and proposed that SnO is formed by

$$Sn + 5OH^- \rightarrow SnO + HSnO_2^- + 2H_2O + 4e^- \quad (3)$$

Further support for this hypothesis was provided by the observation that the ratio of the cathodic to the anodic charge is 0.5 in this voltage region, which also indicates that the oxide is quantitatively reduced. Shah and Davies [20] attributed the negative voltage dip to reduction of an SnO_2 overlayer, which apparently forms at potentials between 0.2 and 1.0 V, inhibits tin dissolution, and causes a reduction in the cathodic/anodic charge ratio.

There is general agreement among workers who have investigated tin passivation in borate solution [19, 20, 22–26] and various other electrolytes [27–41] that SnO_2, or the hydrated species $Sn(OH)_4$, is formed at least at more positive potentials. Negative peaks in chronopotentiograms also have generally been attributed to the presence of an SnO_2 overlayer [8, 20, 27, 28, 33]. The blocking nature of the latter is evident from the results of Nagasaka *et al.* [42] who found that oxidation of SnO at high temperatures (350–600 °C) completely ceases after formation of a thin SnO_2 surface layer. The formation of SnO_2 in electrochemical systems has been confirmed by electron diffraction [8, 29] and Mössbauer spectroscopy [23, 25]. Some workers have attempted to characterize tin surface oxides by Auger electron spectroscopy (AES) and X-ray photoelectron spectroscopy (XPS) but it is not possible to distinguish between SnO and SnO_2 with these techniques [43, 44]. However, application of low energy (75 eV) electron loss spectroscopy (LEELS) has shown conclusively that SnO_2 is involved in even the very early stages of tin oxidation in the gas phase and is enriched in the outer surface as the oxide film grows [44].

Figure 6 shows the effect of anodization voltage limit on the amount of oxide determined by SERA analysis and the wetting times measured at two temperatures for hot-dipped tin specimens. The lower temperature (235 °C) is near the tin melting point (232 °C) so that fusion of the coating would not play a significant role, at least initially. In this case, the wetting time increases relatively little (0.4 to 0.7 s) up to the voltage at which formation of SnO_2 commences (0.2 V), and then increases sharply to a peak of more than two seconds at 0.7 V. Even at the higher temperature (295 °C), which is 63 °C above the tin melting point, this trend is discernible. In contrast, the amount of oxide increases linearly over this voltage range. The most obvious explanation for the concomitant decreases in the wetting time and amount of oxide

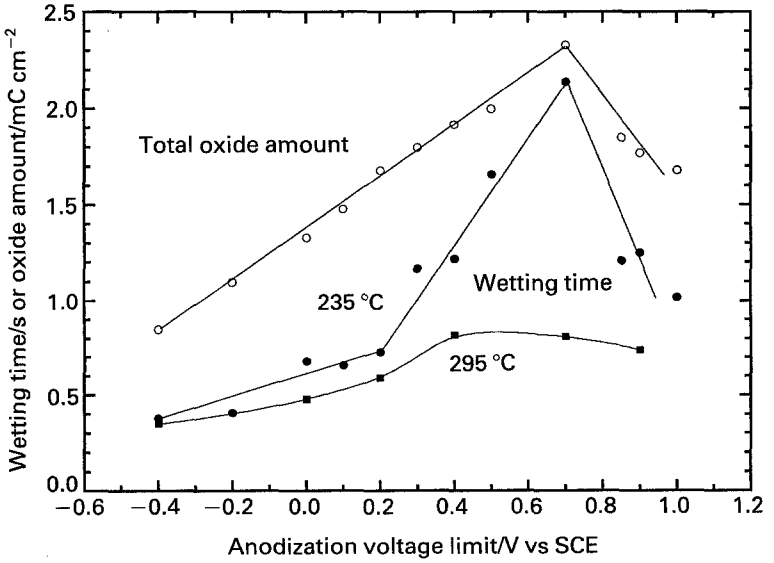

Fig. 6. Plots of the total amount of oxide determined from SERA analysis and wetting times at 235 and 295 °C vs. the positive voltage limit for hot-dipped Sn specimens anodized at 20 μA cm^{-2} in borate buffer solution (pH 8.4).

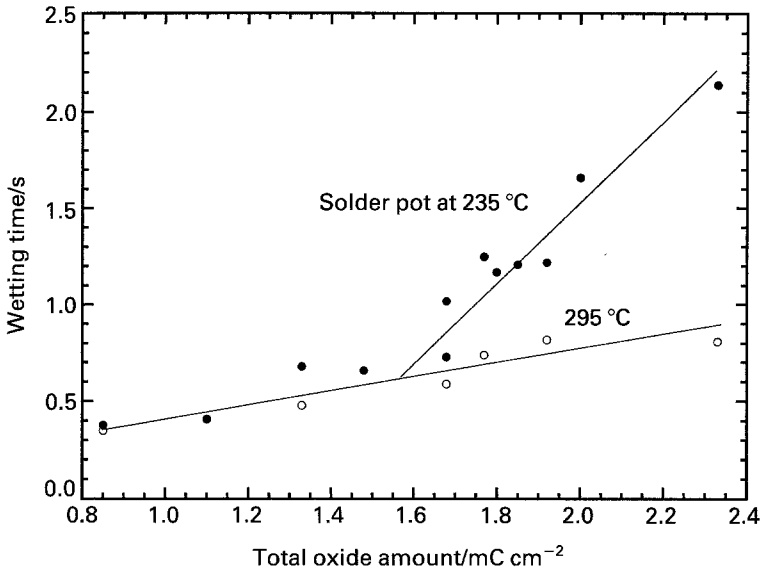

Fig. 7. Plots of wetting time measured at 235 and 295 °C for hot-dipped/anodized Sn specimens vs. the total amount of oxide detected.

detected for anodization voltages positive of 0.7 V is transpassive dissolution of part of the oxide layer. However, formation of a more electrically and thermally conductive oxide that is only partially reduced during SERA analysis is also consistent with the data.

In view of the pronounced change in slope for the wetting time curve, which would be expected to reflect a significant change in the surface oxide, the linear increase in the detected amount of oxide is surprising. In particular, SnO_2 formation beginning at 0.2 V should involve double the charge compared to that for formation of an equal amount of SnO and cause the slope of the oxide amount-voltage limit curve to increase. One explanation of why this does not occur is that SnO_2 forms from SnO and involves simultaneous dissolution according to the following equation:

$$2SnO + 3OH^- \rightarrow SnO_2 + HSnO_2^- + H_2O + 2e^- \quad (4)$$

This disproportionation reaction would be consistent with our data which indicate that the ratio of cathodic to anodic charge is 0.5 ± 0.1 over the entire anodization voltage range from -0.4 to 0.8 V. Shah and Davies [20] did not detect tin in solution above 0.2 V but only one experiment was performed and the accuracy is questionable. A ring-disc electrode study by other workers [45] also indicated that tin dissolution ceases at potentials positive of about 0.0 V. However, the phosphate anion employed in this case is known to participate in the tin passivation process [37] and is likely to suppress tin dissolution.

An alternative explanation for the apparent dichotomy in Fig. 6 is that the amount of SnO_2 is only a small fraction of the total oxide present but has a large effect on the wetting time because it forms a dense layer that is highly resistive. It is also possible that steric factors associated with the growing oxide layer cause SnO to disproportionate chemically to tin and SnO_2 so that the average oxidation state of tin in the oxide film remains constant. Additional work is required to resolve this issue.

Figure 7 shows clearly that the effect of the quantity of oxide on wetting time is small and independent of test temperature when the oxide is predominately SnO (up to about 1.6 mC cm^{-2}). In this case, doubling the oxide amount increases the wetting time by only 0.3 s (from 0.4 to 0.7 s). The fact that the curves for the two temperatures coincide in this region suggests that the wetting time in this case is determined more by the wetting characteristics of the oxide than thermal transfer across the oxide film. The wetting time at the lower temperature increases sharply as the amount of SnO_2 in the surface oxide increases (total oxide amounts above 1.6 mC cm^{-2}), indicating that SnO_2 is much more detrimental to solderability than SnO. In this case, a 50% increase in the total amount of oxide increases the wetting time by about 1.5 s (from 0.7 to 2.2 s).

Additional experiments were performed to demonstrate that some oxide remains on the surface after SERA analysis of specimens anodized at more positive potentials, and to determine the effects of such residual oxide on the wetting time. Specimens anodized to 1.0 V, which increases the hydrogen overvoltage after SERA analysis from -1.3 to -1.45 V (see Fig. 5), were SERA analysed before and after being treated with acidic chromous ion solution to completely reduce the surface oxide. This reduction treatment restored the hydrogen overvoltage (final voltage plateau) to the -1.3 V value characteristic of an oxide-free surface, indicating that residual oxide had been present. This conclusion is supported by the work of Shah and Davies [20] who found that a faint white film, which they attributed to an accumulation of unreduced SnO_2, could be seen on the surface of a tin specimen that had been voltage cycled 8 or 9 times in borate buffer solution.

The effect of this oxide residue was determined by wetting balance tests immediately after SERA analysis for specimens that had been anodized in the

borate buffer. For anodization voltages of −0.2, 0.7 and 1.0 V, the average wetting times (and standard deviations) measured for 5 specimens each after SERA reduction were 0.38 (2%), 0.41 (2%), and 0.47 s (8%), respectively. These times are practically equivalent to the 0.4 s value typical of oxide-free tin surfaces (unanodized and reduced), demonstrating that the effect of the residual oxide is minimal. Because it resists electrochemical reduction, the residual oxide must be patchy and in poor electrical contact with the substrate, which implies that it is also poorly adherent. Such oxide patches that are easily undercut by molten solder would not be expected to greatly affect the wetting behaviour, as observed. These results show that the oxides important to solderability are detected by SERA analysis and a small amount of unreduced oxide does not denigrate the utility of the method. Note that the tin surface oxide formed at less positive anodization voltages, which is more like that formed during natural aging, is apparently reduced fully during SERA analysis.

5. Applicability of SERA method

The SERA method can be applied to almost any part configuration, including both short and long component leads, and circuit board through-holes and surface mount pads. In principle, solderability degradation associated with the oxides of Sn, Pb, Cu, Ag, Fe and Ni can be assessed. At least in some cases, the effects of sulphides can also be determined.

5.1. *Component leads*

Long lead wires are simply immersed, fully or partially, in the deaerated solution, as described above (see Fig. 3). If the cell is not enclosed in an inert atmosphere glove box, the gas exiting the cell should pass through a bubblier so that a positive pressure of inert gas is maintained during the test. For resistors, one wire can be totally immersed (which accurately defines the surface area) and contact can be made to the other wire. In this case, it may be necessary to correct electrode potential measurements for the voltage drop across the resistor. For capacitors, which block the flow of direct current, contact must be made to one end of the wire to be tested. If the contact wire is exposed to the electrolyte, it must be made of a material having a high hydrogen overvoltage (e.g., lead) and the oxide on its surface must be prereduced or taken into account.

Short component leads, e.g. those on a dual-in-line package (DIP), can be tested using the apparatus shown schematically in Fig. 8. A cell having an O-ring seal at the bottom is clamped onto a piece of tin foil supported by a backing plate of a less ductile metal. All cell connections are made through the side of the cell to facilitate changing test specimens. As with other SERA cells, there are provisions for maintaining an inert gas atmosphere and isolating the counter and reference electrodes in separate compartments. The specimen body is attached (via quick drying adhesive) to a plastic or glass rod that can slip through the cell lid, preferably held in a fixed posi-

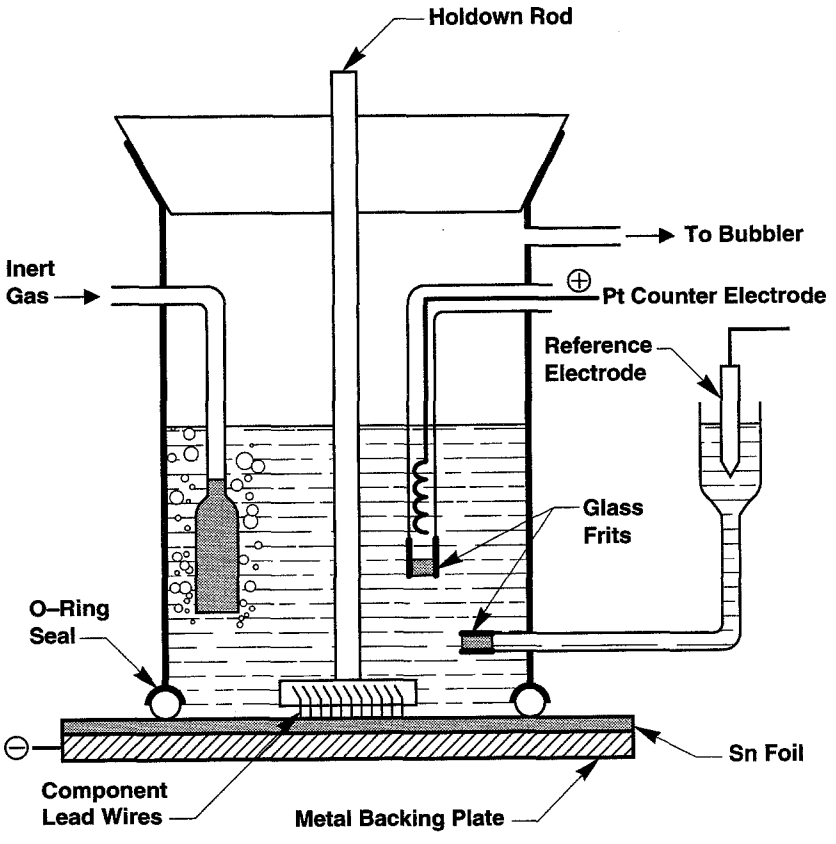

Fig. 8. Cell for SERA testing short component leads.

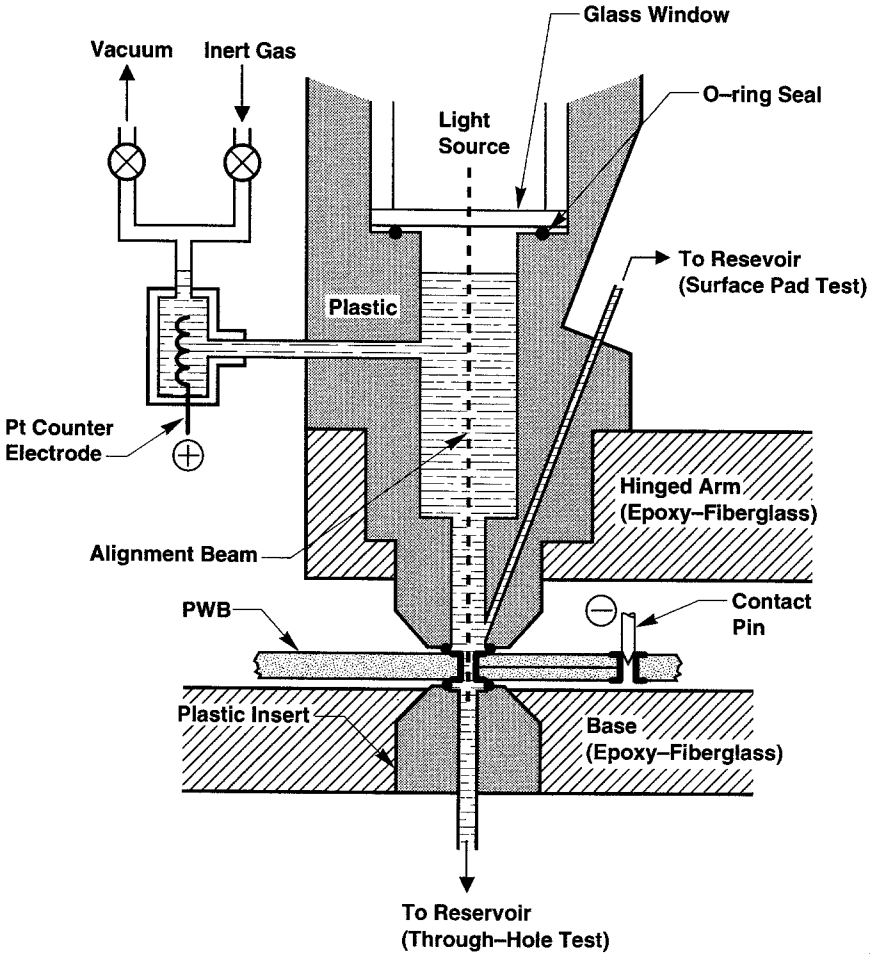

Fig. 9. Apparatus for SERA testing of through-holes and surface pads on printed wiring boards.

tion by an appropriate fitting (not shown). Prior to the test, the specimen is held above the solution and the oxide on the tin foil is prereduced electrochemically so that it does not introduce an error in the measurement. The specimen is then lowered until the leads press firmly against the tin foil and the SERA analysis is performed.

It should be mentioned that a recent publication [46] describes an attempt to analyse oxides on short component leads by electrochemical reduction using a platinum contact. In this case, significant errors associated with concurrent hydrogen evolution, which is catalysed by platinum (as discussed above), are unavoidable. To improve the situation, the authors performed the analysis at constant potential but the currents measured in this case would still include significant contributions from hydrogen evolution and problems associated with incomplete oxide reduction would be exacerbated at the higher current densities involved.

5.2. *Printed wiring boards*

An apparatus for SERA testing of plated through-holes has been applied to analysis of production printed wiring boards [47]. Figure 9 shows a schematic representation of an apparatus for testing either through-holes or surface-mount pads. For through-hole testing, the hinged arm is lowered so that small O-rings (1.6 mm i.d.) form top and bottom seals around the pads of the through-hole to be tested. Alignment is attained via a light beam (as shown) or via a stainless steel centring pin (not shown), which cannot be used for analysis of surface pads and is mounted in a slip fitting in place of the light source. After the apparatus has been purged, electrolyte saturated with inert gas is pulled by a partial vacuum from a reservoir into the upper chamber and counter electrode compartment. Electrical connection is made via another through-hole connected to the one under test. After the analysis, the solution is pushed from the apparatus and through-hole by inert gas. For analysis of surface pads, the electrolyte is introduced and removed via a small hole having one end located very near to the cavity bottom so that solution spillage is minimized.

5.3. *Oxide detection*

Results obtained in our laboratory show that all of the oxides associated with the Sn–Pb–Cu system, including intermetallic oxide species, are readily detected by SERA analysis in borate buffer solution. If anodic tin dissolution which occurs under some conditions is taken into account, cyclic voltammetric studies [9] indicate that analysis of Sn and Pb oxides on tin and Sn–Pb substrates is practically quantitative. Similar

voltammetric studies apparently have not been performed for copper and silver in the borate electrolyte but Campbell and Thomas [2] have shown that their oxides can be quantitatively detected by cathodic reduction in deaerated 0.1 M KCl solution. Since well-defined oxide reduction plateaus have been obtained in our laboratory for copper and silver in borate buffer solution, it is likely that this electrolyte can also be used for SERA analysis of these metals.

Other metals of interest from a solderability standpoint include iron and nickel. Semiquantitative data obtained by Evans, Bannister, and Miley [1] in an open beaker using ammonium chloride solution that had been boiled to remove oxygen demonstrated that chronopotentiometry can be applied to analysis of iron oxides. Recently, Bardwell *et al.* [48] showed that γ-Fe_2O_3 and Fe_3O_4 can be detected on iron in pH 8.4 borate buffer, although simultaneous Fe^{2+} dissolution may render analysis for the former semiquantitative. Okuyama and Haruyama [49] report that NiO and NiO_2 are reversibly produced and reduced electrochemically in pH 8.4 borate buffer, indicating that nickel surfaces can also be analysed in this electrolyte.

These studies indicate that pH 8.4 borate buffer solution could be used for SERA analysis of all of the normally-oxidizable metals currently of importance in electronics manufacturing. However, it is likely that a different choice of electrolyte or pH may be desirable in some cases to enhance detectability of species other than oxides (e.g. sulphides) and/or improve the reversibility of reduction reactions so that voltage plateaus are better-defined. Thus, reduction of recalcitrant oxides, like those of nickel, might be facilitated by use of complexing agents or a lower pH solution. It must be kept in mind, however, that enhanced rates of chemical dissolution and hydrogen evolution in acidic solutions may introduce significant errors in the analysis. One possibility for improving the situation is to add an electrode poison, e.g. arsenate, to the electrolyte to increase the hydrogen overvoltage and thus extend the accessible cathodic voltage range. It should be mentioned that aluminum and titanium oxides are too stable to be reduced electrochemically in aqueous solutions.

5.4. *Sulphide detection*

Metal sulphides resulting from reactions with environmental pollutants or plating bath additives can probably be detected in many cases. Campbell and Thomas [2] found Cu_2S and Ag_2S yield well-defined reduction waves in deaerated 0.1 M KCl solution even when mixed with the respective metal oxide. In practice, the effects of sulphide contamination of solderable finishes may be complicated. Figure 10 shows that exposure of a tin specimen to hydrogen sulphide gas may introduce both a shoulder (onset at about −0.8 V) and a large wave negative of −1.0 V that obscure the features associated with the oxide. Based on this preliminary data, a shoulder at −0.8 V, which is positive of the voltage required for tin oxide reduction, may serve as a flag for sulphide contamination of the surface. Additional work is required to quantitatively relate SERA features associated with sulphides to solderability.

6. Conclusion

The results presented here show that chronopotentiometric detection of surface oxides is a very promising means of nondestructively determining the solderability of metals. It should be emphasized that the goal in SERA analysis (which is chronopotentiometry applied to solderability assessment) is a correlation with solderability parameters rather than the rigorous quantitative detection of surface oxides. Consequently, total separation of the SERA features associated with each oxide and complete oxide reduction are not required. We have found that SERA analysis consistently restores the solderability of both tin

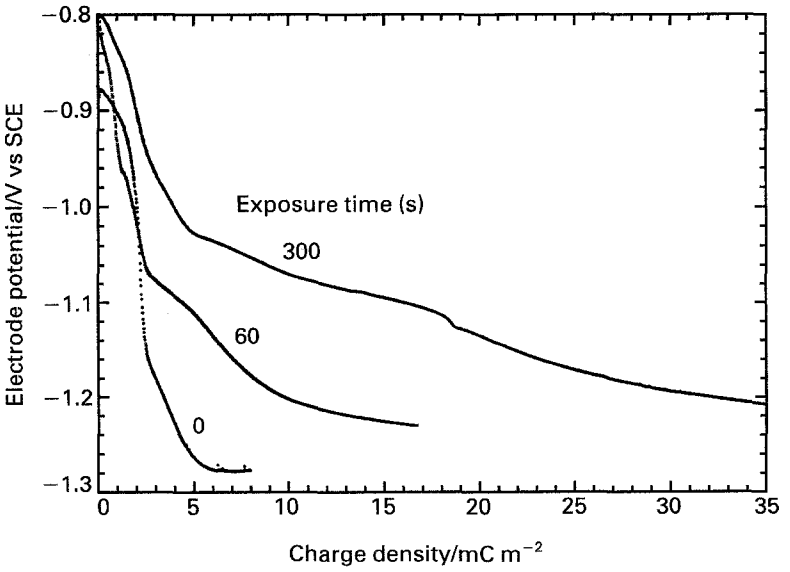

Fig. 10. SERA curves for a hot-dipped Sn specimens with and without exposure to hydrogen sulphide gas for 60 or 300 seconds.

and Sn–Pb specimens to the pre-aged condition, as determined by wetting balance studies involving identical analysed and unanalysed specimens. This is strong evidence that the surface oxides detected by SERA analysis are the primary cause of solderability degradation.

Considerably more work will be required to fully realize the potential of the SERA approach. One impediment is that accelerated aging cannot be counted upon to simulate natural aging processes so that definitive SERA-solderability loss correlations can only be established over relatively long periods of time. A shortcut is to directly establish correlations between SERA data and the occurrence of solderability-related defects for production soldering processes. Such a study involving SERA analysis of printed wiring boards prior to wave soldering has recently been completed and established a correlation between the nature of the oxide on Sn–Pb finishes and the occurrence of soldering defects [47]. Application of SERA testing to metals and alloys other than Cu–Sn–Pb is yet to be explored.

It is encouraging to note that the data reported here for anodized tin actually represents the worst case for applying SERA analysis. From our experience with tin and Sn–Pb finishes, oxides formed slowly by natural aging tend to be composed of intimate oxide mixtures in thinner and less discrete layers that are more readily reduced. Thus, SERA features associated with individual oxide species are usually better defined for naturally-aged specimens. For example, Sn–Pb surfaces not subjected to accelerated aging typically exhibit a small negative peak associated with a very thin outer layer of SnO_2 and a single tin oxide plateau whose voltage shifts to more negative values as the proportion of SnO_2 in the bulk oxide increases and solderability degrades [47]. Results obtained to date for tin and Sn–Pb finishes indicate that the nature of the oxide is more important to solderability than its thickness.

Acknowledgements

The authors gratefully acknowledge the help of Ms Petra Jambazian who performed some of the experiments and are indebted to Dr Martin Kendig for useful comments on the manuscript. This work was performed as part of the Rockwell International IR&D program.

References

[1] U. R. Evans, L. C. Bannister, and H. A. Miley, *Carnegie Schol. Mem., Iron Steel Ins.* **25** (1936) 197.
[2] W. E. Campbell and U. B. Thomas, *Trans. Electrochem. Soc.* **76** (1939) 303.
[3] W. Katz, *Stahl u. Eisen* **76** (1956) 1672.
[4] F. W. Salt and J. G. N. Thomas, *Nature* **178** (1956) 434.
[5] S. C. Britton and K. Bright, *Metallurgia* **56** (1957) 163.
[6] R. P. Frankenthal, T. J. Butler and R. T. Davis, Jr., *Anal. Chem.* **30** (1958) 441.
[7] A. R. Willey and D. F. Kelsey, *Anal. Chem.* **30** (1958) 1804.
[8] S. C. Britton and J. C. Sherlock, *Br. Corros. J.* **9** (1974) 96.
[9] D. M. Tench and D. P. Anderson, *Plating Surf. Finish.* **77**(8) (1990) 44; US Patent pending (filed 28 May 91).
[10] R. J. Bird, *Metal Sci. J.* **7** (1973) 109.
[11] T. Farrell, *Met. Sci.* **10** (Mar. 1976) 87.
[12] R. A. Konetzki, M. X. Zhang, D. A. Sluzewski and Y. A. Chang, *J. Electron. Packaging* **112** (1990) 175.
[13] M. Pourbaix, 'Atlas of Electrochemical Equilibria in Aqueous Solutions', NACE (Cebelcor), Houston (Brussels), 2nd. edn. (1974).
[14] C. I. House and G. H. Kelsall, *Electrochim. Acta* **29** (1984) 1439.
[15] R. Kurz and E. Kleiner, *Z. Werkstofftechnik* **2**(8), (1971) 418; *J. Mater. Technol.* **2,** (1971) 418.
[16] R. P. Frankenthal and D. J. Siconolfi, *J. Vac. Sci. Technol.* **17** (1980) 1315.
[17] R. A. Konetzki, Y. A. Chang and V. C. Marcotte, *J. Mater. Res.* **4** (1989) 1421.
[18] G. V. Samsonov (ed.), 'The Oxide Handbook', IFI/Plenum, New York, (1973) p.263.
[19] S. E. S. El Wakkad, A. M. Shams El Din and J. A. El Sayed, *J. Chem. Soc., Lond.* (1954) 3103.
[20] S. N. Shah and D. E. Davies, *Electrochim. Acta* **8** (1963) 663.
[21] F. H. Howie and E. D. Hondros, *J. Mater. Sci.* **17** (1982) 1434.
[22] M. Pugh, L. M. Warner and D. R. Gabe, *Corros. Sci.* **7** (1967) 807.
[23] A. Vértes, H. Leidheiser, Jr., M. L. Varsányi, G. W. Simmons and L. Kiss, *J. Electrochem. Soc.* **125** (1978) 1946.
[24] I. A. Ammar, S. Darwish, M. W. Khalil and S. El-Taher, *Mat.-wiss. u. Werkstofftech.* **19** (1988) 271.
[25] M. L. Varsányi, J. Jaén, A. Vértes, and L. Kiss, *Electrochim. Acta* **30** (1985) 529.
[26] S. D. Kapusta and N. Hackerman, *ibid.* **25** (1980) 1625.
[27] D. E. Davies and S. N. Shah, *ibid.* **8** (1963) 703.
[28] A. M. Shams El Din and F. M. Abd El Wahab, *ibid.* **9** (1964) 883.
[29] N. A. Hampson and N. E. Spencer, *Br. Corros. J.* **3** (1968) 1.
[30] B. N. Stirrup and N. A. Hampson, *J. Electroanal. Chem.* **67** (1976) 45; **73** (1976) 189.
[31] D. R. Gabe, *Surf. Technol.* **5** (1977) 463.
[32] R. O. Ansell, T. Dickinson, A. F. Povey and P. M. A. Sherwood, *J. Electrochem. Soc.* **124** (1977) 1360.
[33] H. Do Duc and P. Tissot, *Corros. Sci.* **19** (1979) 179.
[34] I. A. Ammar, S. Darwish, M. W. Khalil and A. Galal, *Z. Werkstofftech.* **14** (1983) 330.
[35] I. A. Ammar, S. Darwish, M. W. Khalil and A. Galal, *ibid.* **16** (1985) 194.
[36] I. A. Ammar, S. Darwish, M. W. Khalil and S. El-Taher, *Mat.-wiss. u. Werkstofftech.* **19** (1988) 271.
[37] I. A. Ammar, S. Darwish, M. W. Khalil and A. Galal, *ibid.* **19** (1988) 294.
[38] T. D. Burleigh and H. Gerischer, *J. Electrochem. Soc.* **135** (1988) 2938.
[39] I. A. Ammar, S. Darwish, M. W. Khalil and S. El-Taher, *Corros.* **46** (1990) 197.
[40] B. F. Giannetti, P. T. A. Sumodjo and T. Rabockai, *J. Appl. Electrochem.* **20** (1990) 672.
[41] M. Drogowska, H. Ménard and L. Brossard, *ibid.* **21** (1991) 84.
[42] M. Nagasaka, H. Fuse and T. Yamashina, *Thin Solid Films* **29** (1975) L29.
[43] R. A. Powell, *Appl. Surf. Sci.* **2** (1979) 397.
[44] A. J. Bevolo, J. D. Verhoeven and M. Noack, *Surf. Sci.* **134** (1983) 499.
[45] H. Do Duc and P. Tissot, *Corros. Sci.* **19** (1979) 191.
[46] K.-S. Lei, E. Jones, C. Ramirez, M. Petrucci and J. Kargol, *Proc. NEPCON '92* (1992) 619.
[47] D. M. Tench, M. W. Kendig, D. P. Anderson, D. D. Hillman, G. K. Lucey and T. J. Gher, *Soldering Surf. Mount Technol.,* (13) (Feb, 1993) 46.
[48] J. A Bardwell, B. MacDougall and M. J. Graham, *J. Electrochem. Soc.* **135** (1988) 413.
[49] M. Okuyama and S. Haruyama. *Corros. Sci.* **14** (1974) 1.